Bulletin of Earthquake Engineering (2024) 22:3591–3625
https://doi.org/10.1007/s10518-023-01615-z

S.I. : AI, S AND BDA IN EARTHQUAKE ENGINEERING

# Evolutionary numerical model for cultural heritage structures via genetic algorithms: a case study in central Italy

**Georgios Panagiotis Salachoris[1] · Gianluca Standoli[1] · Michele Betti[2] · Gabriele Milani[3] · Francesco Clementi[1]**

Received: 2 July 2022 / Accepted: 8 January 2023 / Published online: 28 January 2023


## Abstract

In this paper the actual dynamic behavior of the civic Clock tower of Rotella, a little village in central Italy heavily damaged by the recent 2016 seismic sequence, is thoroughly investigated by means of a detailed numerical model built and calibrated using the experimental modal properties obtained through Ambient Vibration Tests. The goal is to update the uncertain parameters of two behavioral material models applied to the Finite Element Model (elastic moduli, mass densities, constraints, and boundary conditions) to minimize the discrepancy between experimental and numerical dynamic features. A sensitivity analysis was performed with the definition of a metamodel to reduce the computational strain and try to define the necessary parameters to use for the calibration process. Due to the high nonlinear dependency of the objective function of this optimization problem on the parameters, and the likely possibility to get trapped in local minima, a machine learning approach was meant. A fully automated Finite Element Model updating procedure based on genetic algorithms and global optimization is used, leading to tower uncertain parameters identification. The results allowed to create a reference numerical replica of the structure in its actual health state and to assess its dynamic performances allowing better control over their future evolution.

**Keywords** Masonry towers · Structural health monitoring · Operational modal analysis · Genetic algorithm · Model updating · Heritage · Uncertainty estimation · Sensitivity analysis

✉ Gabriele Milani
gabriele.milani@polimi.it

[1] Department of Civil and Building Engineering, and Architecture, Polytechnic University of Marche, via Brecce Bianche, 60131 Ancona, Italy

[2] Department of Civil and Environmental Engineering, University of Florence, Via di S. Marta, 50139 Florence, Italy

[3] Department of Architecture, Built Environment and Construction Engineering, Technical University of Milan, Piazza Leonardo da Vinci 32, 20133 Milan, Italy

## 1 Introduction

In the panorama of the structures composing Italian Cultural Heritage (CH), a very vast and relevant field is constituted by masonry towers (Lagomarsino and Cattari 2015; Bartoli et al. 2016, 2017b). The most peculiar feature of these heritage structures comes from their evident slenderness (Bru et al. 2019) which represent a typical vulnerability against the effects of seismic action. For this reason, accurate knowledge of the dynamical parameters that characterize masonry towers is needed to perform any kind of advanced numerical analysis (Gentile and Saisi 2007, 2013; Saisi et al. 2015; Cabboi et al. 2017). These types of analysis became increasingly needed due to the catastrophic earthquakes that stroke Italy the last decades (Umbria–Marche 1997–1998, Abruzzo 2009, Emilia–Romagna 2012, Marche-Lazio-Umbria-Abruzzo 2016–2017) (Formisano et al. 2010). In October 2016, major earthquakes occurred in the Marche region, affecting the entire Centre of Italy, causing widespread damage especially on the Cultural Heritage (CH) structures. Among these important structures, churches, palaces, and towers suffered severe damages and in some instances the entity of the events caused their collapse. The spatial distribution of the events knowing the epicenter stroked the cities of Norcia, Visso, Arquata del Tronto, Accumoli and Amatrice (Poiani et al. 2018; Fiorentino et al. 2018; Clementi et al. 2020). Damages were also reported in the heritage structures from the cities of Tolentino, San Severino, Camerino and Matelica (Chieffo et al. 2019; Ferrante et al. 2021b; Salachoris et al. 2021). This indicated that damages were to be expected in the entire vicinity of the regions and upcoming scenarios and workflows needed to be implemented for conservation and repairing.

The idea of preservation of historical structures has become one of the most studied topics as there are researches that focus on the evaluation of seismic capacity of the structures utilizing diverse tools both physical and numerical, e.g., Operational Modal Analysis, Finite Element (FE) and/or Discrete Element (DE) methods (Sarhosis et al. 2018, 2019; Sarhosis and Lemos 2018). With these tools, it becomes possible to generate highly accurate base models and avoid overestimation of the real capacities that therefore lead to wrong design interventions (Asteris et al. 2015; Ferrante et al. 2021a). To achieve such goal, the tool that is most used in present days is Operational Modal Analysis which aims to identify the real dynamic behavior of the structure. It consists in the registration of accelerometric time-histories produced by only ambient noise (wind, micro-tremors, traffic, etc.) with use of sensors put in the more representative points of the examined structures. The data recorded is subsequently elaborated, cleaned, and analyzed using appropriate algorithms that can extract frequencies, modal shapes, and damping ratios. This kind of operation can be used to satiate different needs: if it is carried out for a short period of time it allows the identification of the parameters, if it is used for long periods, it can be applied for damage detection purposes as any kind of variations in the identified dynamic characteristics can be linked to elasto-geometric or mass variations. Another technique that is used in combination with the Operational Modal Analysis procedures is the FE Model updating, whose application on the design and construction of structures was initially introduced in 1980s and, in recent years, has seen successful applications extended to masonry structures (Milani et al. 2012; Casolo et al. 2013; Formisano et al. 2018, 2021; di Lorenzo et al. 2019; Giordano et al. 2020). This updating process applies to different fields to quantify the uncertainties found on the sensitive properties of a structural system and minimize the distance between numerical and experimental dynamic responses, such as modal frequencies and mode shapes. Although this operation can be performed by trial-and-error approaches,

it results in time consuming operations and becomes quite complex in larger structures making it impossible to receive an accurate estimation of the global optimum solution (Pellegrini et al. 2018). The attention therefore of the researchers turned on towards automated iterative procedures (Bartoli et al. 2017a). These approaches appear to give solutions of a certain degree of confidence but, considering the high computational times required by the elevated numbers of iterations and the difficulty of application when the number of properties is excessive, more approximate procedures are preferred for model updating. Aiming at studying and reducing the number of unknown quantities that are supposed to be considered in the FE model updating, global sensitivity analysis methods can be adopted to effectively measure the dependence between the desired dynamic results (modal frequencies and mode shapes) and the different model properties to better address their selection (Pallarés et al. 2021; Zini et al. 2022). Considering the advantages, the reduction of candidate parameters holds the updating problem to a state that is translated as the actual condition of the structure. Increasing the number of data or changing of the structural conditions implies that the sensitivity analysis must be repeated to avoid ill-conditioned updating states that change the representativeness of the calibrated model, and the considerations that are made in terms of evolution regarding local damage mechanisms. To overcome this aspect, alternative updating methods are considered that can effectively treat large and multi-dimensional problems, such as nature inspired metaheuristics (Girardi et al. 2021).

In this paper, an example of application of automated model updating procedure, coupled to dynamic monitoring activity and modal parameters identification process is presented, applied to the case study of the Clock Tower of Rotella, a small town sited in the Marche region (Central Italy). The work is organized as follows:

- In Sect. 2 the results of the geometric and material surveys of the tower are presented;
- Section 3 is dedicated to modal identification process, starting from the description of the monitoring campaign and presenting the results of the application of OMA techniques to the acquired data in order to extrapolate the modal characteristics (frequencies and mode shapes) which are going to be the targets for the updated FE model;
- Section 4 is focused on the main theme of the work, so the calibration process of the FE model, realized recurring to a combined approach based on sensitivity analysis and Genetic Algorithm (GA) for the automatic tuning of the numerical model material parameters. The GA is implemented thanks to the open-source solver Code_Aster©, found in the Openturns/Persalys software (Baudin et al. 2015) contained in Salome-Meca© environment. After considering the influence of the different quantities on the reproduction of the structural dynamic behavior into the model, both isotropic and orthotropic material approach have been evaluated.
- At least, Sect. 5 summarizes the results of the analysis, proposing two sets of mechanical parameters (one for every material approach considered) which allow the FE model to reproduce the effects highlighted by the monitoring activities.

## 2 Clock tower of Rotella: description of the case study

### 2.1 Historical survey

Rotella (Fig. 1a) is a small town of the Marche region (Central Italy), specifically located in Ascoli Piceno province, an area dramatically affected by the seismic events of 2016. The

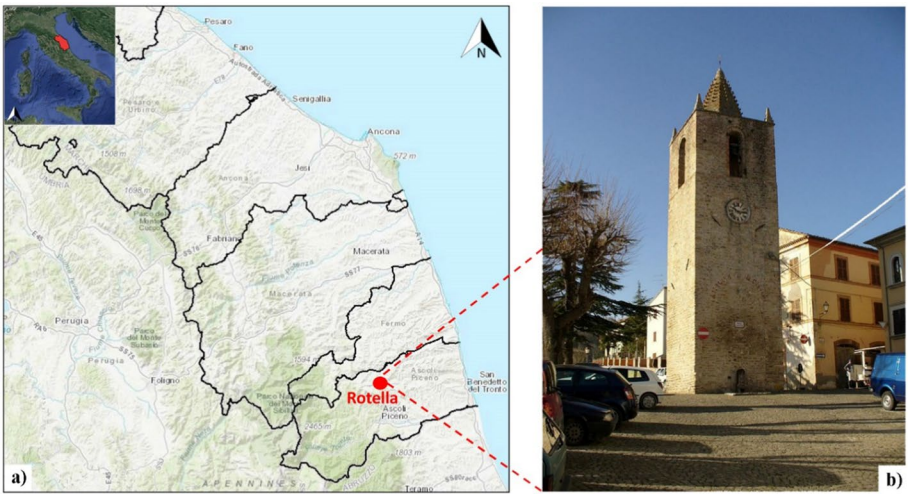


**Fig. 1** Rotella Village (**a**), and a view of the tower (**b**)

city name comes from the latin word "Rota", meaning "wheel", probably inspired by the circular shape of the terrace where the city arises. All around the landscape is characterized by Ascensione Mountain, once called "Monte Nero" (in English, "Black Mountain") because of the thick forest which covers the ground, and two rivers, respectively Tesino River and its tributary Oste River.

Rotella Clock Tower (Fig. 1b) stands as an isolated masonry structure, sited in the city center. Till 1755, it was part of the former church of "Santa Maria della pietà", destroyed in that year because of a landslide.

During the ages the Tower, as well as the rest of the city, has been struck by several earthquakes, even of high entity, among which, the more recent ones are L'Aquila, in 2009, that incredibly did not affect the structure, and the seismic sequence of 2016- '17 which instead severely damaged the building, as testified by the smeared cracks which propagated near the bell-cell openings (Ferrante et al. 2021a).

## 2.2 Geometrical and material survey

The clock tower is defined by a square section of dimensions $4.60 \times 4.65$ m$^2$ with masonry bearing walls of 1 m thickness built with irregular stones, except for the N-E wall (Fig. 2) that has a reduced thickness of 0.6 m for the first meters of height. The construction is composed of three floors. Masonry floor slab is found at ground level, while aged wood composes the upper floors. The ground floor slab is made of masonry while the others are made of aged wood. The bell-cell features a double-arched window on the S-W side, while the other three facades have single-arched windows. The cell is covered by an octagonal shaped dome.

During the visual inspection of the tower damaged parts were noticed. Those parts concerned mainly the inner part of the Nort-East and North-West facades (Fig. 3). The cracks observed seemed important enough and a probable cause other than age for their appearance is deducted to be the Central Italy event. Those parts during the modelling restitution were considered as discontinuities of the geometry.

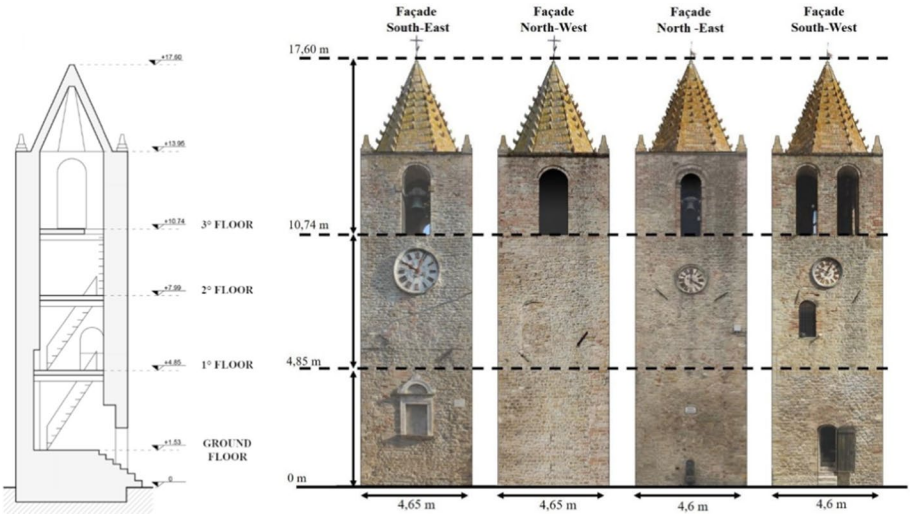


**Fig. 2** Rotella Civic Tower prospect representation and section

**Fig. 3** Damages of the North-East and North-West walls of the Rotella Civic Tower

## 3 Ambient vibration testing

Simplicity of the installation, relative economy of the instrumentation, possibility to not interrupt the buildings operativity are some of the main features which bestowed popularity

to the use of Ambient Vibration Testing (AVT) in global dynamic behavior of CH structures assessment (Brincker et al. 2000; Benedettini et al. 2015, 2017). Once the most sensitive points of a structure are individuated, experimental data can be easily collected just placing a set of sensors, minimizing the risk of affecting the historical value of the building and the goods therein contained like other diagnostic techniques can do. The analysis of the vibrational data, so acquired, enables the possibility to characterize the system response to the random excitations (environmental or anthropic) it is subdued (Saisi et al. 2016; Pierdicca et al. 2019; Azzara et al. 2021). In particular, the most significant dynamic features of the system, namely natural frequencies ($f$), damping ratios ($\xi$) and mode shapes ($\varphi$), can be extracted, and used to better interpret the actual behavior of age-old constructions, which are often highly complex and mechanically diverse.

Recent years field literature is full of works, based both on short- and long-time approaches, whose results proved the effectiveness of vibration monitoring through accelerometric sensors and of the application of the known identification methods. In fact, by processing these data it is possible to build an Experimental Model (EM) of the structure, which provides the dynamic parameters that the Numerical Model (NM) must match to realistically reproduce the structural response (Ubertini et al. 2016, 2017, 2018; Kita et al. 2019). This approach provided useful information about the dynamic behavior and the health status of a great number of real operative structures, very important for their current and future preservation.

### 3.1 Field testing procedure

To identify the dynamic behavior of the Clock Tower of Rotella a field-testing campaign, under operational conditions, was conducted in 2018. It is noted that the sensor layouts for signal acquisition were established considering the optimal placement in accordance with a preliminary modal analysis of the structure, maximizing the quality of the AVT responses despite the use of limited available sensors. Four triaxial Piezo-MEMS accelerometers, synchronized by a Sync-HUB connected to a portable station (Milani and Clementi 2021; Standoli et al. 2021a), were deployed in the points showed in (Fig. 4), going to form the sensors network for the monitoring of the building. Each registration lasted 45 min. A sampling rate of 1024 Hz was set for data recording of the 8 different measurement points, for a total of 24 nodal processes of nearly 3 million datapoints per channel.

A number of setups equal to four was adopted during the campaign to measure the tower's response. For each of the setups, the four accelerometers were positioned in the corners of the structure, always keeping the two in the corners of the last elevation as reference, and evenly distributing the others downward the height of the tower. This allowed the registration of the vibrations of the selected corners in the three principal spatial directions, catching their most meaningful modal displacements, including those related to the torsional component.

### 3.2 Operational modal analysis

#### 3.2.1 Data processing

Acceleration time series, collected with the modalities exposed in the previous paragraph, have been processed applying the well-known Operational Modal Analysis Techniques (OMA), to execute the dynamic identification of Rotella Tower. Even though a vast set

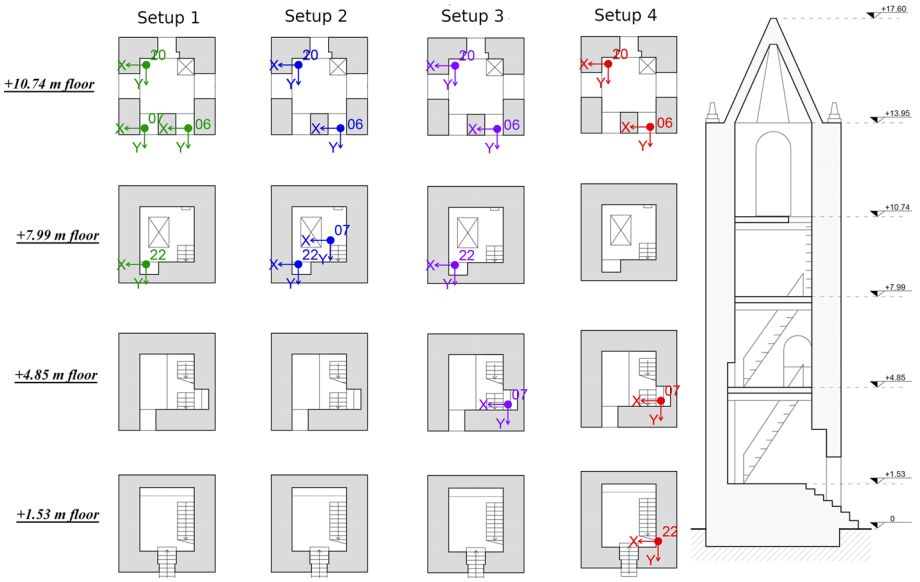


**Fig. 4** Sensor locations of the AVT procedure

of approaches are available in the field of output-only analysis, applicable both in time than frequency domain (Benedettini et al. 2015, 2017). All of these approaches converge over the necessity of operating a pre-process stage over the measurement before the adoption of the extrapolation strategy chosen by the user. This step is required to free the data from eventual residual noise components or polynomial trends, to reduce possible persistent leakage errors, to eliminate undesired frequencies ranges, and so to minimize all the effects which could corrupt the identification process. Also, down-sampling can be applied in this stage, reducing the frequency range of interest for the structure and consequently the computational costs.

A script implemented in Matlab© was able to manage the pre-processing of data. At first a linear detrend of data was executed; immediately after, a 10th order Butterworth low-pass filter was used over the raw signals. Then, the data deprived of excessive noise contents were downsampled to the frequency range between 0 and 12.5 Hz, which is considered the one of interest for the case structure. This operation required the use of a decimation factor pair to 8, which lead the spectral resolution from 1024 to 100 Hz. Finally, elaborated signals were subdued to the commercial software ARTeMIS©, where a module for modal parameters extraction through the Stochastic Subspace Identification (SSI) method is available.

### 3.2.2 Theoretical background on SSI–based methods

When a modal identification process needs to be carried out, users can recur to methodologies working in frequency or in time domain (Ewins and Saunders 1986), depending on the purposes of the investigation and the characteristics of data. In cases like the one under analysis, where the modes to be identified tends to be closely spaced, the adoption of time domain techniques tends to be preferable. Among the possible approaches present in time

domain category, the most used is the Stochastic Subspace Identification (SSI) method (Peeters and de Roeck 1999).

Considering the dynamic of a linear-time-invariant system subjected to unknown excitation source, whose dynamic behavior is described recurring to the well-known second order differential equation of motion, this method assumes the construction of a State Space model where the problem is converted into a set of two independent linear equations. For a State Space assumed as *discrete in time*, the aforementioned equations, respectively known as "state equation" and "observation equation", can be expressed as in Eqs. (1) and (2):

$$\boldsymbol{x}_{k+1} = \boldsymbol{A}\boldsymbol{x}_k + \boldsymbol{w}_k \tag{1}$$

$$\boldsymbol{y}_k = \boldsymbol{C}\boldsymbol{x}_k + \boldsymbol{v}_k \tag{2}$$

where: $k$ is the generic time instant; $\boldsymbol{x} \in \mathcal{R}^{nx1}$ is the discrete-time state vector; $\boldsymbol{y} \in \mathcal{R}^{lx1}$ is the vector containing the $l$ output measurements; $\boldsymbol{A} \in \mathcal{R}^{nxn}$ is the system matrix that describes all the dynamic information of the system; $\boldsymbol{C} \in \mathcal{R}^{lxn}$ is the corresponding output matrix; $\boldsymbol{w} \in \mathcal{R}^{nx1}$ is a white noise vector process representing disturbances and modelling inaccuracies; $\boldsymbol{v} \in \mathcal{R}^{lx1}$ is another white noise vector process representing the measurement noise due to sensor inaccuracy.

Two implementations are disposable for applying the method:

- the Covariance-driven (SSI-cov) approach, where the modal estimation is executed through the Singular Value Decomposition (SVD) of the Toeplitz block matrix of the covariances of the elements contained in the acquired time series;
- the Data-driven (SSI-data) approach, implemented in various commercial software (like ARTeMIS©), which operates the SVD of the Hankel matrix, so a block matrix composed by past and future output measurements.

An uncertainty factor, common to both identification techniques, stands in the selection of a correct model order for a reliable estimation of the system dynamic response. It is common to overcome this problem by recurring to the so called "*stabilization diagrams*", which are charts, having frequencies on abscissas and model order on the ordinate axes, where all the possible stable solutions are reported for increasing model order. As concerns the maximum model order it is normally assumed as higher than two times the number of modes to be identified. Among all the possible solutions, represented as poles, those associated to zero or negative damping ratios are discarded as well as those exceeding the maximum gap in terms of standard deviation among modal parameters of two successive model orders. The remaining poles, considered stable and characterized by vertical alignment for a given frequency value in the chart, are accounted as the investigated structural modes for the analyzed system.

### 3.2.3 Modal identification results

The identification process terminated with the extrapolation of the modal characteristics associated to five vibration modes located in the frequency range 0–12.5 Hz. For both the dynamic testing campaign the results (Fig. 5) show two modes ($\varphi_1$ and $\varphi_2$), respectively translating in x and y direction, showing modal frequencies values close between themselves, having a gap of 3.94%. The third mode ($\varphi_3$) results torsional, while a bending

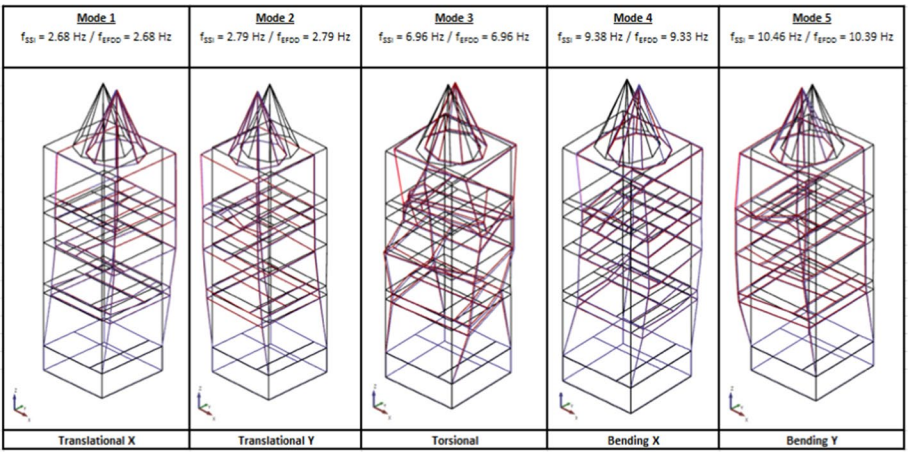


**Fig. 5** Mode shape correlation between the SSI and EFDD approaches of the identification scheme

component characterizes the modes $\varphi_4$ and $\varphi_5$, which are respectively flexural in xz and yz planes. To be noted the high value of the first two modes, which far exceed the classical outcome expected for masonry towers, whose motivations can be probably associated to the low aspect ratio ($\lambda = 4$) exhibited by the tower.

All the modal parameters identified, and selected as targets for the following calibration process, are reported in Table 1, where a third column reporting the corresponding Mode Complexity Factor (MCF) is present. As concerns this last parameter, it consists of a scalar value, often expressed as percentage, comprised between 0 and 100%, which quantifies the level of complexity possessed by the mode, so how much the mode shape vector differs from an only real valued one. The value of 0% indicates a mode close to a real-valued one, while 100% is associated to a completely complex mode. For all the identified modes, the MCFs result low, indicating the modes are practically monophasic. The higher levels are found in correspondence of the 3rd and 4th mode, but this aspect can be probably reconducted to a low level of excitation of the structure during the monitoring campaign.

The goodness of the identification outcome has also been verified through a cross examination applied between the mode shapes identified with time domain techniques and those coming from the application of a frequency domain method, known as Enhanced Frequency Domain Decomposition (EFDD) (Jacobsen et al. 2006). This comparison has been carried out using a well-known methodology, based on the so-called Modal Assurance Criterion (MAC), which consists in a statistical tool which evaluates the consistency

**Table 1** Stochastic Subspace Identification frequency, damping and complexity results

| Frequency (Hz) | ξ (%) | MCF (%) |
|---|---|---|
| 2.68 | 1.344 | 2.089 |
| 2.79 | 1.084 | 0.282 |
| 6.96 | 1.505 | 2.088 |
| 9.38 | 3.618 | 3.966 |
| 10.46 | 1.416 | 0.228 |

of modes, calculating the level of similarity between the mode shapes vectors identified for the different approaches. Good/perfect correspondence is associated to a MAC matrix formed by terms near the unity on the principal diagonal, while terms near to zero indicates the orthogonality of the considered mode shapes. Being the comparison operated between different models, CrossMAC indicator has been used (Pastor et al. 2012).

The mode shapes of the identified parameters are shown in Fig. 5, while in Table 2 are shown the result of the application of the MAC criterion.

## 4 Sensitivity analysis and uncertainty estimation

Heritage structures exhibit extremely variable dynamic behaviors, due to the intrinsic complexities and uniqueness which characterize every single building, which are linked to the constructive typology, materials, and events the structure under analysis has been subdued in its life. A methodology which produced good results in terms of accuracy of the buildings condition assessment consists in the combination of FE modeling with OMA identification techniques, updating the matrices defining the system to minimize the gap between numerical and experimental information. This procedure can be executed manually (Torres et al. 2017; Standoli et al. 2020) or, following the actual trend, in automatic way (Girardi et al. 2020; Standoli et al. 2021b).

The generation of a model apt to be used for damage identification and localization is not an easy task, even with the levels reached nowadays in the field of model update. Having said that there needs to be a high degree of reliability in the model's construction, both in terms of geometrical and structural forms, so that it is possible to capture both local than global behaviors in a realistic way.

Once these features were considered, another uncertainty that must be deeply studied, since it strongly affects the updating process, is the selection of the correct number of parameters to be considered. This choice needs to guarantee a well-conditioned problem, independent of the state of the structure and easily replicable under quasi-real-time conditions to evaluate possible global and local changes in respect to the reference dynamic properties. The determination of such parameters with reasonable initial values, together with the definition of their upper and lower limitations, plays an important role to the convergence and physical consequence of the final updated parameters. With a mindful eye in those considerations and the model updating technique another step must be performed before the final definition of the number of parameters to take into consideration, that of a sensitivity analysis (Pellegrini et al. 2018).

**Table 2** CrossMAC for the correlation between the SSI and EFDD mode shape results of the identification procedure

| CrossMAC | EFDD | | | | |
|---|---|---|---|---|---|
| | 2.68 Hz | 2.79 Hz | 6.96 Hz | 9.33 Hz | 10.39 Hz |
| SSI | | | | | |
| 2.68 Hz | 99.60% | 1.10% | 3.20% | 57.70% | 0.01% |
| 2.79 Hz | 1.20% | 99.60% | 0.36% | 2.80% | 45.00% |
| 6.96 Hz | 3.40% | 0.20% | 98.50% | 21.70% | 0.30% |
| 9.38 Hz | 55.70% | 1.90% | 20.00% | 98.40% | 1.00% |
| 10.46 Hz | 0.01% | 45.70% | 1.20% | 1.70% | 95.50% |

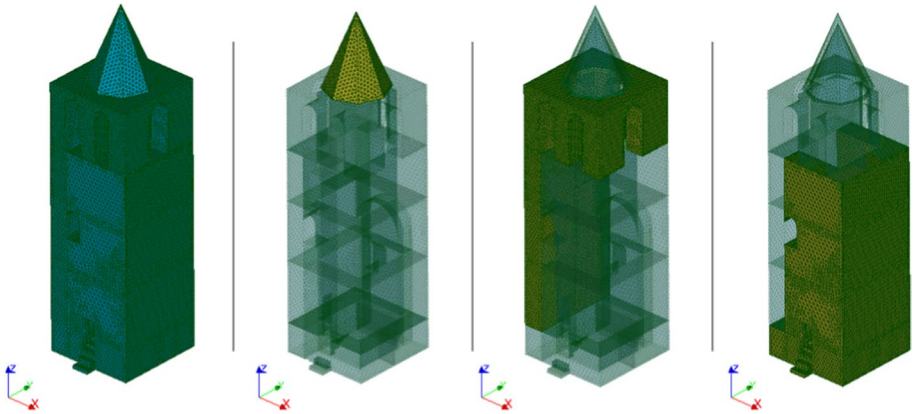

**Fig. 6** The preliminary discretization applied for the first modal analysis of the Rotella Civic Tower

**Table 3** Preliminary analysis material values considering the isotropic behavioral model

| Material | E (MPa) | $\nu$ (−) | $\gamma$ (kN/m$^3$) |
|---|---|---|---|
| Masonry | 1050 | 0.25 | 18 |

### 4.1 Preliminary FE model

The first step in the understanding of the dynamic behavior of the tower consists in the building of a 3D FE model of the structure, where the geometry and the mechanical characteristics are defined. The working environment is Salome-Meca© 2021, where a module, dedicated to geometry definition, can be found. As already stated in the previous paragraph, geometry is one of the parameters which more influences the global response of the structure, so particular attention has been paid to its construction. This means that all the features, whose presence was considered important in the dynamic response of the tower, such as openings, wall thicknesses, irregularities, etc., have been modelled. Also, the recognition of damage in some areas of the building, due to the action of meaningful events or simply due to ageing, has been considered and reproduced in the 3D model: it is the case of the damages highlighted over the North-East and South-East facades. For the final geometry of the model a mesh composed of tetrahedral elements with 0.3 m in size is used. This led to a discretization accounting for 34,659 nodes for the 143,516 volume elements adopted, corresponding to a total of 108,957 DOFs. The static scheme assumed for the structure is that of the cantilever beam, reproduced applying rigid constrains at the basement of the model.

The preliminary modal analysis was run considering an *isotropic* and then an *orthotropic* models for materials. At first a three materials groups discretization was applied (Fig. 6), where the initial not calibrated values of Young's Modulus (E), Poisson's ratio ($\nu$) and mass density ($\gamma$) were chosen according to the Italian Law (Ministero delle infrastrutture e dei trasporti 2019). The initial values assumed for both material approaches are reported in Tables 3 and 4.

Speaking about the dependence of the results upon mesh refinement and typology of FEs utilized, it is interesting to point out that an initial sensitivity analysis was

**Table 4** Preliminary analysis material values considering the orthotropic behavioral model

| Material | $E_{L,N,T}$ (MPa) | $G_{L,N,T}$ (MPa) | $\nu_{LN,LT,TN}$ (−) | γ (kN/m$^3$) |
|---|---|---|---|---|
| Masonry | 1050 | 1050 | 0.25 | 18 |

performed by varying the mesh size within the same finite element typology. Authors experienced that the results obtained are quite insensitive from the discretization adopted. In support of such a conclusion, it should be noted also that the models are created and analyzed in different software platforms, an approach which corroborates the idea to rate the results obtained not affected by issues related to the particular choice made on the typology of FEs used.

Another important issue to consider with particular care would be the soil-structure interaction. Indeed, the influence of soil and foundation conditions in the dynamic behavior of a structure is a feature well known from the literature of the field, and may play an important role in the frequencies determination. However, due to the lack of specific information regarding the soil structure and the state of the foundations (which was not subdued to specific tests), it was impossible to consider this aspect in the analysis and the classic cantilever beam scheme, usually adopted in field works, was hypothesized.

Modal analysis, based on Lanczos implementation, were carried out on the preliminary FE models, allowing a first generic evaluation of the differences in the responses between the numerical and the experimental models (Girardi et al. 2021).

Starting with the NM considering isotropic material, the results obtained for the first five modes are reported in Table 5, where it is possible to see how, apart for the first mode, the variations between EM and NM frequencies are quite low, with a perfect correspondence for the second mode.

Concerning the mode shapes, satisfactory results are shown correlating the displacements of the two models. In fact the modes $\varphi_1$ and $\varphi_2$ respectively kept x and y as rigid direction of motion, mode $\varphi_3$ presents a strong torsional connotation, and also good correspondence is found for the last two flexural modes, respectively oriented towards x and y direction (Fig. 7).

The comparison between the experimental and preliminary numerical mode shapes of the isotropic behavioral model was performed with the MAC index, showing a fair correlation between the fundamental modes of the tower, while higher modes detail a decreasing correlation as is shown in Table 6.

Different results are those regarding the modal analysis operated over not calibrated orthotropic model, where also five modes are identified, but the differences between

**Table 5** Modal results of the preliminary modal analysis considering the isotropic behavioral model and comparison between the experimental and numerical frequency values

| Mode N | $f_{exp}$ (Hz) | $f_{num}$ (Hz) | Mass X (%) | Mass Y (%) | $\Delta f_{exp\text{-}num}$ (%) |
|---|---|---|---|---|---|
| $\varphi_1$ | 2.68 | 2.17 | **54.91** | 1.71 | **19.03** |
| $\varphi_2$ | 2.79 | 2.79 | 1.73 | **53.96** | 0.00 |
| $\varphi_3$ | 6.96 | 7.05 | 0.00 | 0.00 | **1.29** |
| $\varphi_4$ | 9.34 | 9.58 | **17.53** | 0.01 | **2.57** |
| $\varphi_5$ | 10.47 | 10.21 | 0.00 | **18.00** | **2.48** |

Main modes and the differences between experimental and numerical models are highlighted in bold

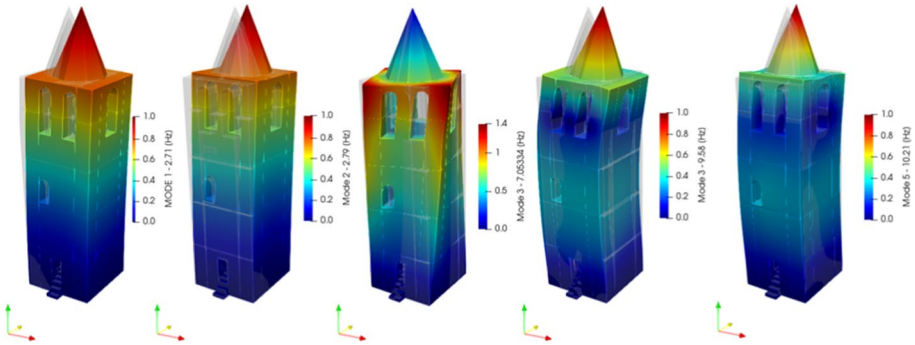


**Fig. 7** Preliminary mode shapes for the isotropic behavioral model

**Table 6** CrossMAC between the uncalibrated preliminary NM and the SSI identification results concerning the mode shapes

| CrossMAC | Isotropic behavioral model | | | | |
|---|---|---|---|---|---|
| | 2.17 Hz | 2.79 Hz | 7.05 Hz | 9.58 Hz | 10.21 Hz |
| SSI | | | | | |
| 2.68 Hz | 94.55% | 6.09% | 7.33% | 59.90% | 1.85% |
| 2.79 Hz | 3.66% | 93.89% | 0.00% | 0.57% | 35.27% |
| 6.96 Hz | 5.35% | 3.42% | 97.77% | 39.24% | 10.62% |
| 9.38 Hz | 63.27% | 0.20% | 14.43% | 90.36% | 1.46% |
| 10.46 Hz | 0.29% | 51.97% | 4.06% | 1.22% | 85.53% |

**Table 7** Modal results of the preliminary modal analysis considering the orthotropic behavioral model and comparison between the experimental and numerical frequency values

| Mode N | $f_{exp}$ (Hz) | $f_{num}$ (Hz) | Mass X (%) | Mass Y (%) | $\Delta f_{exp\text{-}num}$ (%) |
|---|---|---|---|---|---|
| $\varphi_1$ | 2.68 | 2.95 | **51.76** | 2.72 | **10.07** |
| $\varphi_2$ | 2.79 | 2.99 | 2.74 | **50.94** | **7.17** |
| $\varphi_3$ | 6.96 | 10.36 | 0.00 | 0.07 | **48.85** |
| $\varphi_4$ | 9.34 | 11.47 | **17.88** | 0.00 | **22.81** |
| $\varphi_5$ | 10.47 | 12.21 | 0.00 | **17.43** | **16.62** |

Main modes and the differences between experimental and numerical models are highlighted in bold

experimental and NM -in terms of eigenvalues- show bigger gaps, with the maximum value in correspondence of the third mode (Table 7).

More correspondence is found in the comparison of the eigenvectors, whose main displacement components are coincident with those extrapolated for the experimental model, as it possible to observe in Fig. 8 and from the values of the main diagonal of the MAC matrix, reported in Table 8.

The preliminary results show a better correspondence between the experimental model and the NM which considers the material as isotropic, while it is to see how bigger the error is in the comparison with the orthotropic behavioral model, for which the gap increases moving towards the higher modes. This kind of error is probably related to the number of

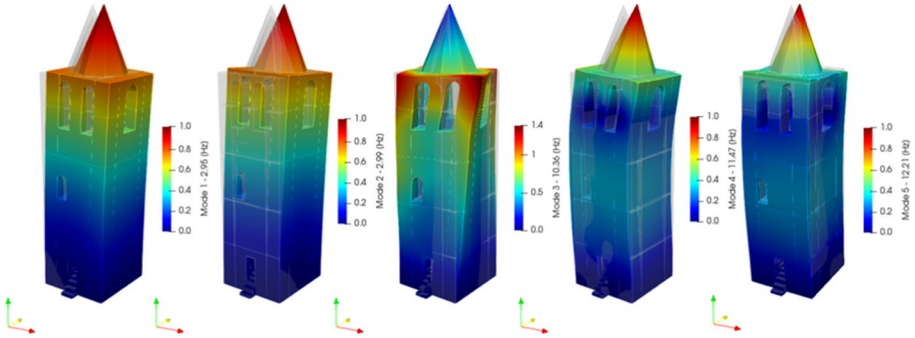


**Fig. 8** Preliminary mode shapes for the Orthotropic behavioral model

**Table 8** CrossMAC between the uncalibrated preliminary model and the SSI identification results concerning the mode shapes for the orthotropic behavioral model

| CrossMAC | Orthotropic Behavioral Model | | | | |
|---|---|---|---|---|---|
| | 2.95 Hz | 2.99 Hz | 10.36 Hz | 11.47 Hz | 12.21 Hz |
| SSI | | | | | |
| 2.68 Hz | 91.89% | 8.88% | 7.22% | 58.13% | 2.61% |
| 2.79 Hz | 5.71% | 91.12% | 0.07% | 1.32% | 32.91% |
| 6.96 Hz | 3.68% | 4.89% | 96.80% | 36.90% | 14.11% |
| 9.38 Hz | 69.05% | 0.14% | 14.83% | 88.91% | 1.16% |
| 10.46 Hz | 0.72% | 57.82% | 1.74% | 0.46% | 76.72% |

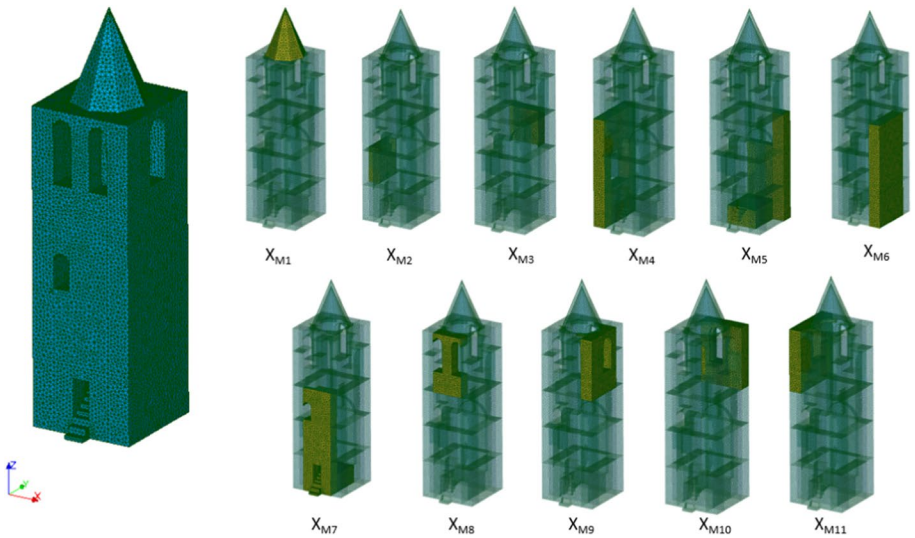


**Fig. 9** Eleven discretization representation

groups used for the initial discretization, which results too low for the orthotropic model to faithfully adapt to the experimental model dynamic behavior.

A further step is considered before the updating procedure to study the models' parameters uncertainty and sensitivity considering higher discretization schemes (Fig. 9) to account for the visible variability of the masonry properties and damage across the Clock Tower. Due to the high computational needs, a surrogate procedure was applied to reduce the computational strain.

### 4.2 Metamodel

The high number of variables to be considered in the model updating process drastically increases the computational strain required for a successful calibration of a 3D FE model, leading to the well accepted practice of recurring to the so called "*metamodels*" (Forrester and Keane 2009; Lejeune 2021). Metamodels, which are also known as "*surrogate models*" (Queipo et al. 2005), are a way to represent a physical system as a "*data model"*, connecting specific set of inputs, describing the real system, to outputs in the virtual one.

For a model, named "*F*", whose behavior is representable through a vector $x = (x_1, x_2, x_3 \dots x_n) \in R$, the response $Y$ can be described as:

$$Y = F(x) \tag{3}$$

where $F : R^N \rightarrow R^M$.

Once the metamodel is built, and the dependencies between inputs and outputs are defined, it is possible to use this tool to examinate the influence that each parameter has in the updating process, based on the values of the calculated Sobol's Indexes (SIs), for both the material approaches. This process is known as *sensitivity analysis* (Cheng et al. 2020) and is very common to be used to decrement the computational costs, decrementing parameters number subjected to the model updating process (Saltelli 2002).

From a practical point of view, the transition from FE model, realized through Midas FEA©, to metamodel is possible through a specific toolkit present in Code_Aster© environment. The main steps of this conversion are listed below:

(1) NM and EM are initially imported and read by Code_Aster©, where a condensed experimental model (CEM) containing the frequency and mode shape data belonging to the five estimated modes are created;
(2) CEM data are projected onto the NM to upscale the EM DOFs. This operation enables the possibility to visualize and interact with the data onto a 3D model while also creating the dependencies for the displacement calculations between the existing nodes of the NM with respect to the data of the EM;
(3) Once the projection is obtained, a preliminary modal analysis is performed, generating the initial population for the values of the unknown material properties to be considered in the calibration process;
(4) Upper and lower bounds of physical significance are also set for each updating parameter based on values retrieved from the literature and belonging to analogous structures. Any value within the bounds is a candidate solution.

The experiment is designed following a probabilistic approach (Sacks et al. 1989), where 1024 samples are considered for the analysis to be run. The sample generation is entrusted to a Monte-Carlo algorithm. For each of the considered parameters, an initial

**Table 9** Parameter initial values, lower and upper bounds considering also values for the damaged part of the model applied to the isotropic behavioral model

| Parameters /Bounds | Initial value | Lower bound | Upper bound |
|---|---|---|---|
| E (Mpa) | 1000 | 300 | 3100/1000 |
| $\nu$ (−) | 0.25 | 0.2 | 0.45 |
| ρ (kN/m$^3$) | 18 | 18 | 20.0 |

**Table 10** Parameter initial values, lower and upper bounds considering also values for the damaged part of the model applied to the orthotropic behavioral model

| Parameters /Bounds | Initial value | Lower bound | Upper bound |
|---|---|---|---|
| $E_{L,N,T}$ (MPa) | 1000 | 300 | 3100/1000 |
| $G_{L,N,T}$ (MPa) | 1000 | 300 | 1400 |
| $\nu_{LN,LT,TN}$ (−) | 0.25 | 0.2 | 0.45 |
| ρ (kN/m$^3$) | 18 | 18 | 20 |

value and a range of variation is imposed, applying a normal distribution. Moreover, to reproduce the real structural behavior as faithfully as possible, the eventual presence of damage, resulting from the material surveys, was considered in the definition of the initial values for the iterative procedure, and for establishing the lower and upper bounds. These input parameters are reported in Tables 9 and 10.

The criteria for the acceptance of the results consider both the outcome in terms of eigenvalues than of eigenvectors. Similarities can be noticed between the two behavioral models' uncertainty estimation (Tables 11 and 12) both regarding their statistical estimates and with the correlation matrix.

The differences found are caused by the elevated number of unknowns of the orthotropic model. Despite those differences, an interesting trend is noticed in the correlation between the first and second MAC diagonal values of both behavioral models (Fig. 10).

The understanding of the trend shows that the correlation between the first two fundamental modes is locked, so when the values of the sample are differently distributed along the models' discretization, the first mode tends to become the second and vice versa. The same trend is not manifested so clearly in the correlation between the first and the other eigenvectors.

The metamodel was created following a Kriging approach (García-Macías et al. 2020), which is a methodology coming from Geostatistic, and it consists in a technique to interpolate spatial data. The final goal of the procedure is the definition of a predictor denoted as $\hat{G}$, which is considered as an outcome of the normal process $Y : \Omega \times R^d \rightarrow R$, defined by:

$$Y(\omega, x) = f(x) + F(\omega, x) \tag{4}$$

where: $f(x)$ defines the trend; $F(x, \omega)$ is a zero-mean Gaussian process with a covariance function $C : R^d \times R^d \mapsto R$ dependent on the vector of parameters $x \in R$.

The validation of the metamodel (Tables 13 and 14, Figs. 14 and 15), which denotes its capability to reproduce the observed outcome, was done by selecting three different

**Table 11** Uncertainty quantification for the isotropic behavioral model considering 1024 samples

| | $\Phi_1$ | $\Phi_2$ | $\Phi_3$ | $\Phi_4$ | $\Phi_5$ | $\Phi_{1NM}/\Phi_{1EM}$ | $\Phi_{2NM}/\Phi_{2EM}$ | $\Phi_{3NM}/\Phi_{3EM}$ | $\Phi_{4NM}/\Phi_{4EM}$ | $\Phi_{5NM}/\Phi_{5EM}$ |
|---|---|---|---|---|---|---|---|---|---|---|
| Mean | 3.21 | 3.39 | 7.97 | 11.22 | 11.91 | 0.92 | 0.92 | 0.98 | 0.88 | 0.73 |
| Sx | 0.18 | 0.18 | 0.37 | 0.48 | 0.53 | 0.08 | 0.07 | 0.01 | 0.06 | 0.10 |
| CV | 0.06 | 0.05 | 0.05 | 0.04 | 0.04 | 0.09 | 0.08 | 0.01 | 0.07 | 0.13 |
| Skewness | − 0.16 | − 0.10 | − 0.24 | − 0.16 | − 0.18 | − 2.42 | − 1.59 | − 3.05 | − 2.14 | − 1.63 |
| Kurtosis | 2.95 | 2.98 | 3.01 | 3.01 | 3.14 | 11.28 | 6.62 | 20.31 | 14.21 | 7.26 |
| First quartile | 3.10 | 3.27 | 7.74 | 10.89 | 11.57 | 0.89 | 0.88 | 0.98 | 0.86 | 0.68 |
| Third quartile | 3.34 | 3.51 | 8.24 | 11.56 | 12.27 | 0.98 | 0.97 | 0.98 | 0.92 | 0.80 |

**Table 12** Uncertainty quantification for the orthotropic behavioral model considering 1024 samples

| | $\Phi_1$ | $\Phi_2$ | $\Phi_3$ | $\Phi_4$ | $\Phi_5$ | $\Phi_{1NM}/\Phi_{1EM}$ | $\Phi_{2NM}/\Phi_{2EM}$ | $\Phi_{3NM}/\Phi_{3EM}$ | $\Phi_{4NM}/\Phi_{4EM}$ | $\Phi_{5NM}/\Phi_{5EM}$ |
|---|---|---|---|---|---|---|---|---|---|---|
| Mean | 3.42 | 3.60 | 10.02 | 12.60 | 13.33 | 0.80 | 0.81 | 0.97 | 0.86 | 0.75 |
| Sx | 0.19 | 0.17 | 0.32 | 0.42 | 0.38 | 0.24 | 0.22 | 0.03 | 0.07 | 0.08 |
| CV | 0.05 | 0.05 | 0.03 | 0.03 | 0.03 | 0.30 | 0.27 | 0.03 | 0.08 | 0.11 |
| Skewness | − 0.46 | − 0.21 | − 2.98 | − 0.63 | − 0.03 | − 1.71 | − 1.75 | − 26.39 | − 5.25 | − 4.45 |
| Kurtosis | 4.23 | 2.89 | 43.78 | 5.14 | 2.97 | 4.88 | 5.40 | 77.22 | 45.56 | 36.11 |
| First quartile | 3.30 | 3.49 | 9.84 | 12.35 | 13.07 | 0.77 | 0.77 | 0.97 | 0.85 | 0.72 |
| Third quartile | 3.55 | 3.72 | 10.22 | 12.86 | 13.60 | 0.96 | 0.95 | 0.98 | 0.90 | 0.79 |

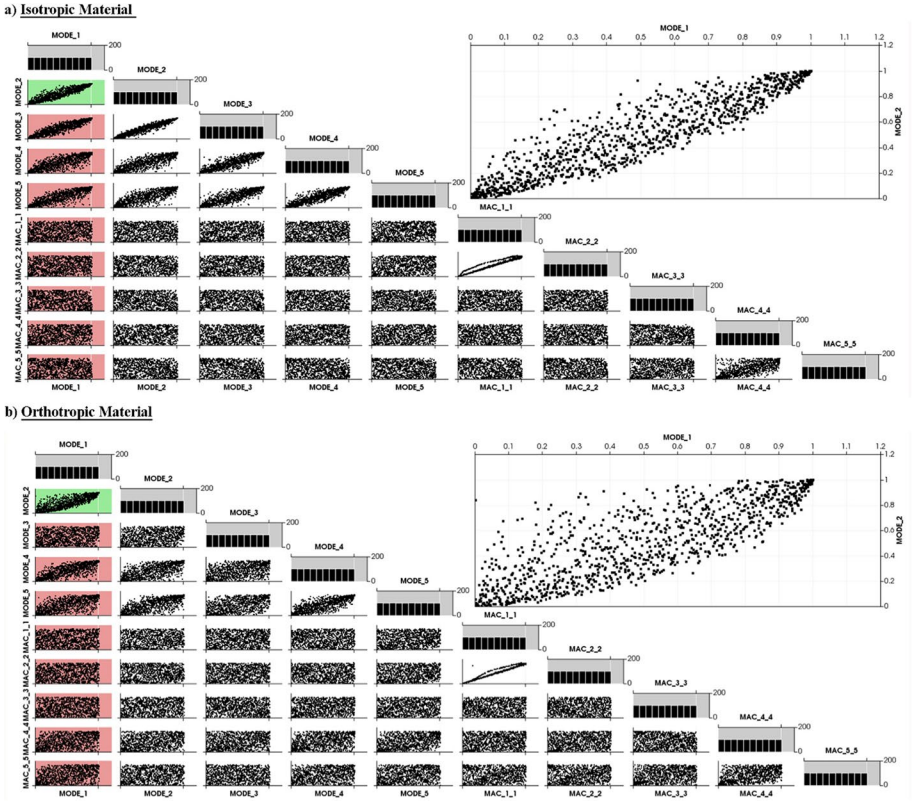


**Fig. 10** Frequency correlation matrix and diagonal MAC values of the isotropic behavioral model (**a**) and orthotropic behavioral model (**b**)

approaches and, as acceptable estimate, the $R^2$ index. The validation solutions were provided as follows:

1. analytically (Figs. 11a and 12a);
2. by dividing the dataset in an 80/20 per cent scheme, were 80% (820 samples) were taken as training data ad 20% (204 samples) as validation (Fig. 11b and 12b);
3. using a K-fold procedure using 10 numbers of folds (Fig. 11c and 12c). This last technique relies on the division of the dataset in K mutually exclusive subsamples. A subsample each time is set aside for the metamodel to be built on the remaining ones.

The validation of the metamodel dwells in acceptable limits for the eigenvalue results for both the isotropic and orthotropic models. The eigenvector predictor is found to provide different results between the two behavioral models because the variety of the sampled values, that the orthotropic model considers, is affected differently in contrast to the isotropic counterpart, due to the higher number of unknowns and

**Table 13** Validation for the isotropic behavioral model considering 1024 samples

| | $\Phi_1$ | $\Phi_2$ | $\Phi_3$ | $\Phi_4$ | $\Phi_5$ | $\Phi_{1NM}/\Phi_{1EM}$ | $\Phi_{2NM}/\Phi_{2EM}$ | $\Phi_{3NM}/\Phi_{3EM}$ | $\Phi_{4NM}/\Phi_{4EM}$ | $\Phi_{5NM}/\Phi_{5EM}$ |
|---|---|---|---|---|---|---|---|---|---|---|
| Number of points | 1024 | | | | | | | | | |
| Number of folds | 10 | | | | | | | | | |
| R2 Analytical validation | 100% | 100% | 99% | 99% | 99% | 96% | 96% | 80% | 84% | 92% |
| R2 Test/Train validation | 99% | 100% | 99% | 100% | 100% | 96% | 96% | 82% | 79% | 91% |
| R2 K-fold validation | 100% | 100% | 99% | 99% | 99% | 95% | 96% | 81% | 84% | 91% |

**Table 14** Validation for the orthotropic behavioral model considering 1024 samples

| | $\Phi_1$ | $\Phi_2$ | $\Phi_3$ | $\Phi_4$ | $\Phi_5$ | $\Phi_{1NM}/\Phi_{1EM}$ | $\Phi_{2NM}/\Phi_{2EM}$ | $\Phi_{3NM}/\Phi_{3EM}$ | $\Phi_{4NM}/\Phi_{4EM}$ | $\Phi_{5NM}/\Phi_{5EM}$ |
|---|---|---|---|---|---|---|---|---|---|---|
| Number of points | 1024 | | | | | | | | | |
| Number of folds | 10 | | | | | | | | | |
| R2 Analytical validation | 88% | 96% | 69% | 81% | 92% | 43% | 41% | − 11% | 12% | 17% |
| R2 Test/Train validation | 91% | 96% | 86% | 89% | 95% | 37% | 32% | − 523% | − 4% | 10% |
| R2 K-fold validation | 88% | 96% | 80% | 81% | 92% | 42% | 39% | − 234% | 6% | 14% |

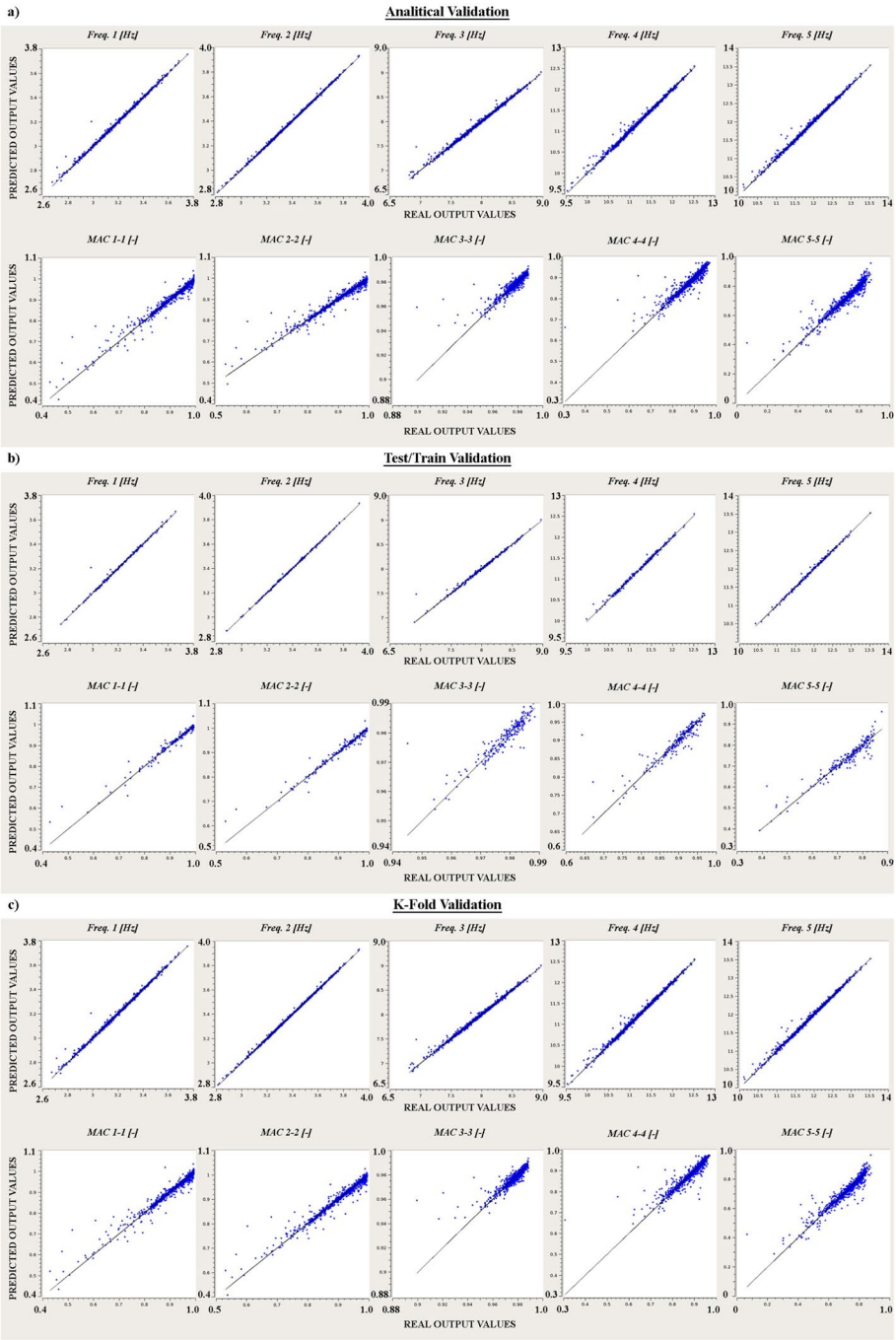


**Fig. 11** Validation process considering modal frequencies and MAC values for the isotropic behavior approach: analytical validation (**a**), test/train validation (**b**), K-Fold validation (**c**)

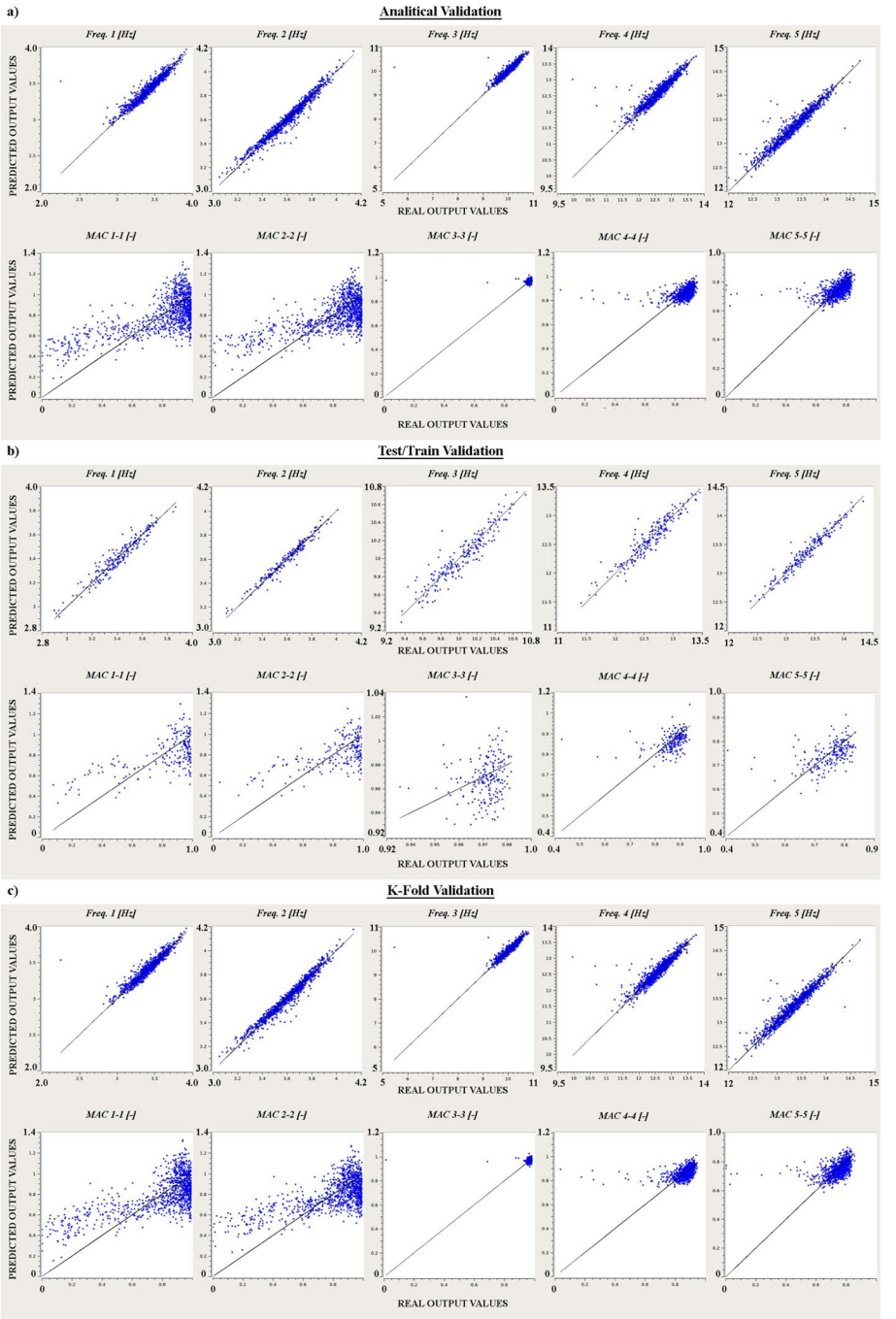


**Fig. 12** Validation process considering modal frequencies and MAC values for the orthotropic behavior approach: analytical validation (**a**), test/train validation (**b**), K-Fold validation (**c**)

complexity it provides in the analysis. The complexity of both models and their results is enhanced along with the discretization selected for the Clock Towers modelling.

### 4.3 Sensitivity analysis

The sensitivity analyses (Arwade et al. 2010; Sun and Dias 2021), in the current study, are aimed to evaluate how the variation of a parameter influences the response of the model in terms of modal frequencies and mode shapes. This evaluation is executed for both material approaches, calculating the values of the SI, defined in Eq. (5):

$$SI_{ik} = \left| \frac{X_k}{Y_i} \cdot \frac{\Delta Y_i}{\Delta X_k} \right| \cdot 100 \tag{5}$$

where: $X_k$ is the *k-th* uncertain parameter; $Y_i$ is the *i-th* predicted parameter; $\Delta$ the variation produced in the relevant parameter.

In the analysis of SIs behavior two conditions are considered, respectively called "First Order Index", which considers the response obtained varying every single parameter by 100%, and "Total Order Index", which considers the effect on the response considering the relation with other parameters variation. For both isotropic and orthotropic material approaches, the results of sensitivity analysis on Elastic Modulus (Figs. 13a and 14a), Poisson's ratios (Fig. 13b and 14c) and mass density (Figs. 13c and 14d), and only for the orthotropic case on the Shear Modulus (Fig. 14b), are shown.

The sensitivity First order and Total indexes indicate an increased activity regarding the perturbation of the modulus of elasticity for the material values applied at the discretization $X_{M3}$ and $X_{M6}$, that are the parts afflicted by damage as was seen during the visual survey, a mediocre activity for the ones of $X_{M5}$ and $X_{M7}$, while decreased activity is noticed for the rest along both behavioral models.

### 4.4 Nature-inspired model updating

The NM updating problem presents itself in the environment of Structural Health Monitoring (SHM) in the form of an inverse problem based on modal analysis. Iterative procedures aim at providing solution to this inverse problem by calibrating the FE model by applying corrections to the mechanical parameters that dictate the models' functionality. This calibration is guided by an objective function whose purpose is to filter out the non-optimal solutions and search for the global optimum by minimizing the distance between experimental and numerical modal data. In order to withdraw also from manual iterative applications of calibrating schemes, a Genetic Algorithm (GA) (Bianconi et al. 2020; Standoli et al. 2021b) was applied implemented in Code_Aster© software environment to proceed with the automatic calibration of the Civic Tower of Rotella. Inspired by Darwin's Evolutions theory, they are methods which try to reproduce the way in which generations propagates in nature, so naturally selecting the best characteristics for future development. They are considered very reliable tools in the resolution of optimization problems, allowing the possibility of evaluating the same problem from different perspectives, always aiming to the search of global optimum, but discarding the risk of being stuck in local minima.

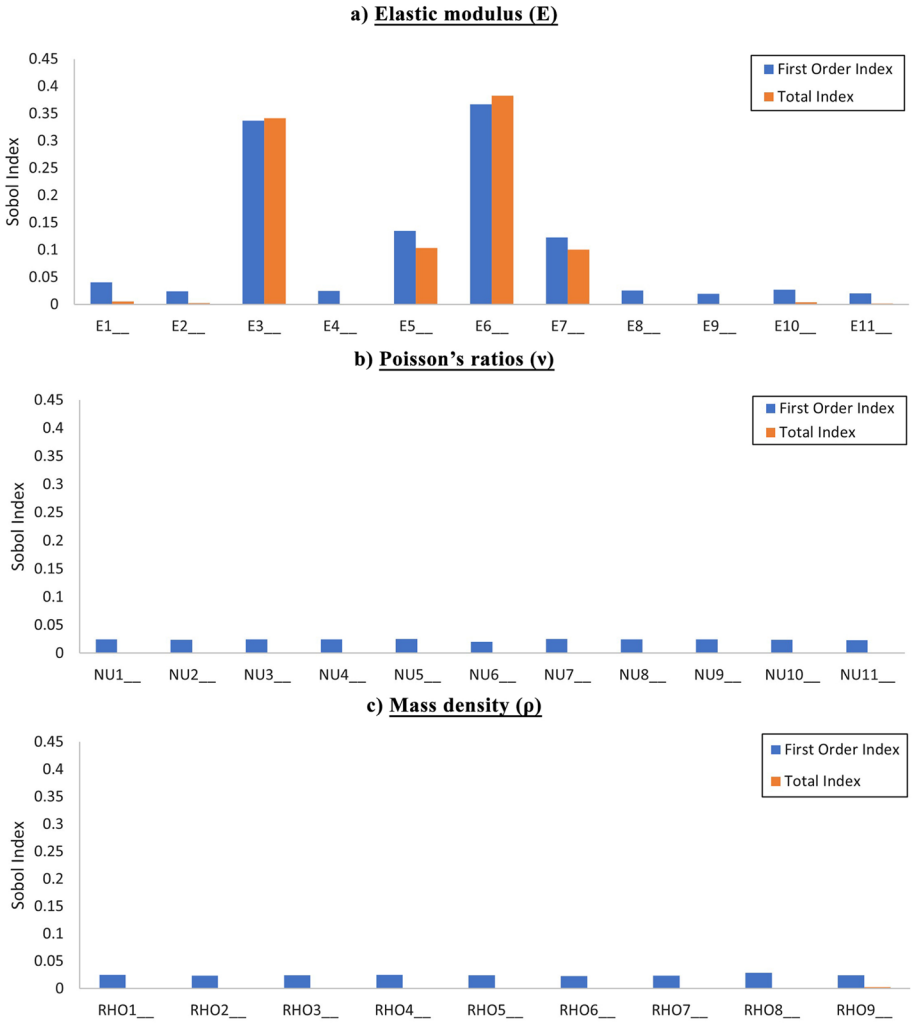


**Fig. 13** Sensitivity analysis with First Order (in blue) and Total Order (in orange) of Sobol Indices calculated over perturbation of Elastic Modulus (**a**), Poisson's ratios (**b**) and Mass density (**c**) for the isotropic material

### 4.4.1 Calibration process

The workflow of the calibration procedure through GA is illustrated in Fig. 15 (Standoli et al. 2021b). For the first step the NM and EM are imported and read by Code_Aster©. Into this environment the experimental data are projected over the NM to upscale the EM DoFs. An intermediary NM, containing the frequency values and mode shapes of the EM, is generated, also enabling the possibility to visualize and interact with the data and create dependencies for the calculations between the existing nodes of the NM in respect to the EM.

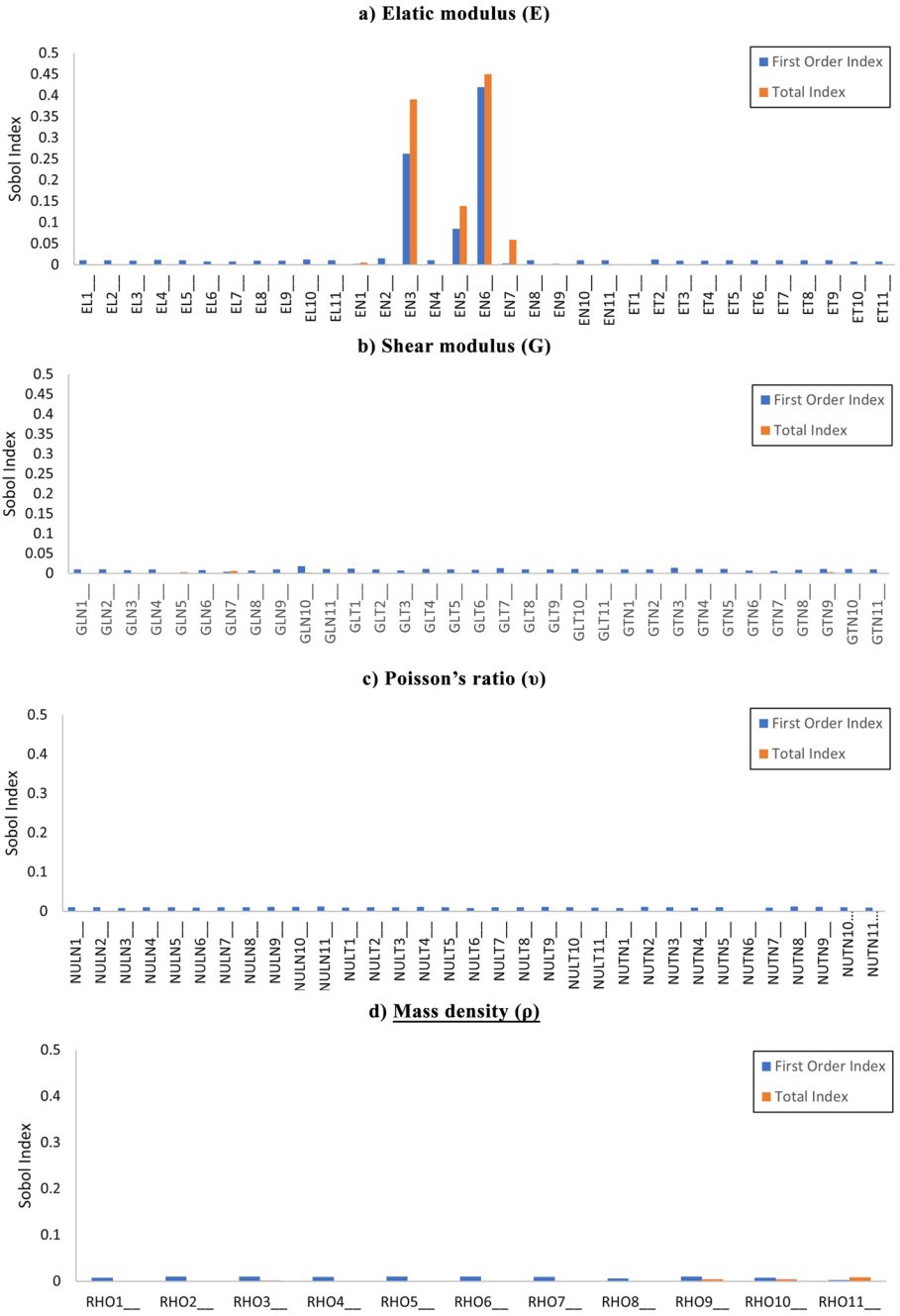


**Fig. 14** Sensitivity analysis with First Order (in blue) and Total Order (in orange) of Sobol Indices calculated over perturbation of Elastic Modulus (**a**), Poisson's ratios (**b**) and Mass density (**c**) for the orthotropic material

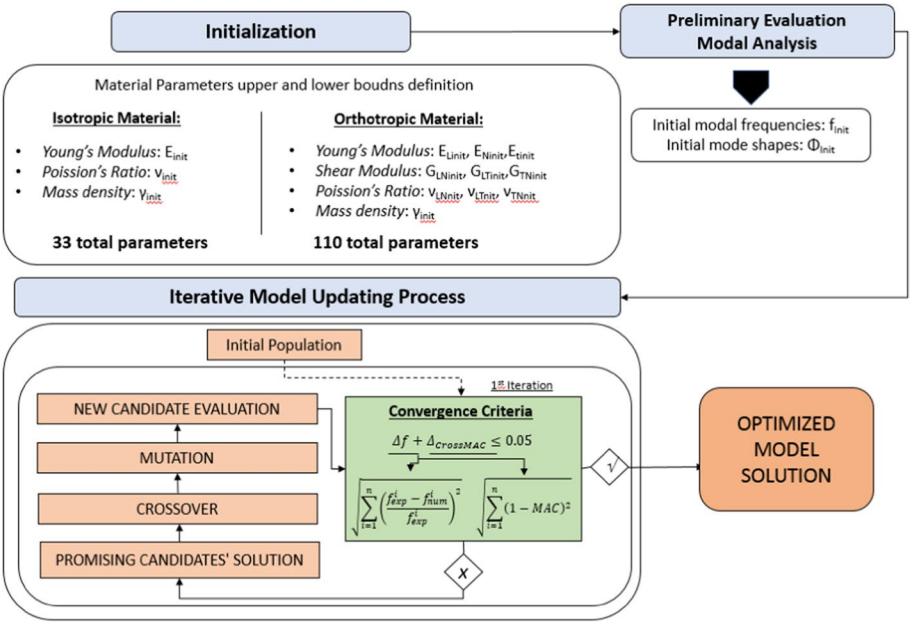


**Fig. 15** Genetic Algorithm workflow representing the parameters of the isotropic and orthotropic behavioral models

Once the intermediary model is generated, a preliminary modal analysis is performed to create an initial population for the values of the material properties. Considering the sensitivity and uncertainty analyses results, the same bounds for the different parts of the discretization were applied. Any value in the limits of bounds was considered a viable solution. The size of the population to be initialized in each iteration of the algorithm is given by the parameter called "NB_PARENTS", initially set to 10. In the first stage, only one evaluation is made to define the initial error measurement. In each successive evaluation, a parameter "NB_FILLS" manages the number of iterations. The larger this parameter is, the larger the renewal of the population is made although as a drawback a higher computational cost is required. Once the number of parents and individuals is defined, then in each iteration of the algorithm, the fulfilment of convergence criteria established is checked using a two-term objective function (Magalhães et al. 2009; Ceravolo et al. 2016; Standoli et al. 2021a, b) that accounts for both eigenvalues and eigenvectors residuals between the EM and NM, as:

$$\Delta f + \Delta_{crossMAC} = \sqrt{\sum_{i=1}^{n}\left(\frac{f_{exp}^{i} - f_{num}^{i}}{f_{exp}^{i}}\right)^{2}} + \sqrt{\sum_{i=1}^{n}\left(1 - MAC^{i}\right)^{2}} \leq 0.05 \tag{6}$$

Limits to the tolerance allowed between two consecutive step (equal to $1e^{-4}$) and over the maximum number of evaluations (pair to 2000) are imposed, comporting the stop of the updating process if the limits are exceeded. If not, elaborations proceed until the achievement of a stable solution.

**Table 15** Frequency results of the isotropic behavioral model considering two standard deviations for the GA and the differences between the results

| Mode | $f_{EXP}$ (Hz) | $f_{NM02}$ (Hz) | $f_{NM05}$ (Hz) | $\lvert\Delta f_{EM\text{-}NM}\rvert$ σ = 0.2 | $\lvert\Delta f_{EM\text{-}NM}\rvert$ σ = 0.5 |
|---|---|---|---|---|---|
| $\Phi_1$ | 2.68 | 2.78 | 2.72 | 3.73% | 1.49% |
| $\Phi_2$ | 2.79 | 2.80 | 2.79 | 0.36% | 0.00% |
| $\Phi_3$ | 6.96 | 6.91 | 6.90 | 0.72% | 0.86% |
| $\Phi_4$ | 9.34 | 9.44 | 9.43 | 1.07% | 0.96% |
| $\Phi_5$ | 10.47 | 10.2 | 10.26 | 2.58% | 2.01% |

**Table 16** Frequency results of the orthotropic behavioral model considering two standard deviations for the GA and the differences between the results

| Mode | $f_{EXP}$ (Hz) | $f_{NM02}$ (Hz) | $f_{NM05}$ (Hz) | $\lvert\Delta f_{EM\text{-}NM}\rvert$ σ = 0.2 | $\lvert\Delta f_{EM\text{-}NM}\rvert$ σ = 0.5 |
|---|---|---|---|---|---|
| $\Phi_1$ | 2.68 | 2.64 | 2.68 | 1.49% | 0.00% |
| $\Phi_2$ | 2.79 | 2.68 | 2.79 | 3.94% | 0.00% |
| $\Phi_3$ | 6.96 | 7.56 | 7.06 | 8.62% | 1.44% |
| $\Phi_4$ | 9.34 | 9.70 | 9.47 | 3.85% | 1.39% |
| $\Phi_5$ | 10.47 | 10.45 | 10.37 | 0.19% | 0.96% |

During the process, the best individual parent is drawn from the population according to a Tournament selection method. A uniform crossover operator is applied to combine the genetic information of two parents and generate new children. The particularity of the uniform crossover operator is that it takes with equal probability the information. All the operations are controlled by the value of the parameter of the standard deviation (ECART_TYPE) defined as:

$$\sigma = \sqrt{\frac{\sum_{i=1}^{N} \left(x_i - \mu\right)^2}{\mathrm{N}}} \tag{7}$$

where: $x_i$ is the i-*th* value from the population; $\mu$ is the population mean; the denominator N stands for the population size.

For the present study, the value of the parameter ECART_TYPE was initially defined as 0.5 and changed to 0.2 to see its application in a narrower search space. The replacement of the older population is controlled by the sum of the parents and that of the children (NB_PARENTS + NB_FILLS). During this implementation said value was set at 15. A hierarchy is created between the individuals according to the values associated during the calculus and the current population gets replaced with the best parent found amongst the global population.

The purpose of the nature-inspired model updating procedure, considering initially 33 variables (isotropic behavioral model) and then 110 variables (orthotropic behavioral model), was to produce and refine to a limit reaches a baseline model as representative of the experimental target that would eventually be updated with new data, and serve as evolutionary numerical model of the existing structure. Another scope of this procedure was to see in what length can the GA calibrate a structure in which damage is modelled not considering non linearities or damage models.

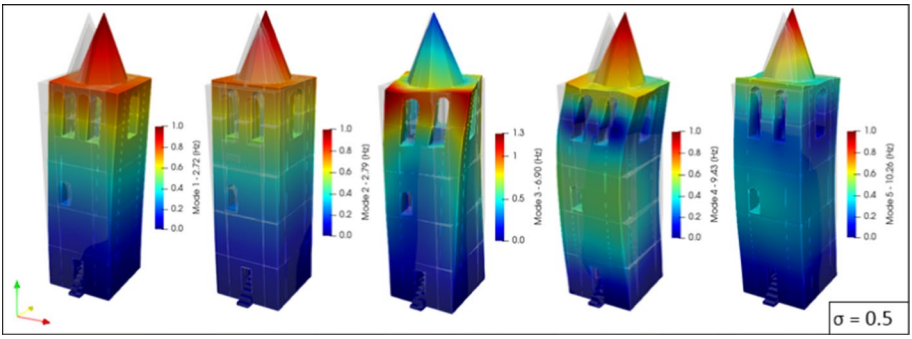


**Fig. 16** Isotropic behavioral calibrated mode shapes with standard deviation of 0.5

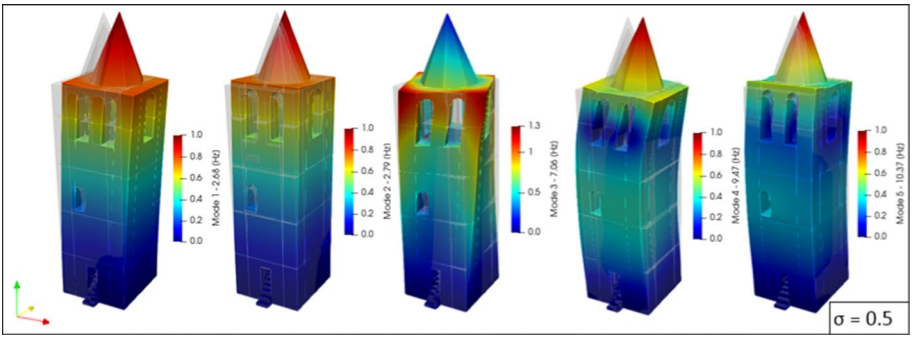


**Fig. 17** Orthotropic behavioral calibrated mode shapes with standard deviation of 0.5

### 4.4.2 Model updating results

Tables 15 and 16 report the results, in terms of frequencies, coming from the application of GA based procedure for the model updating of Rotella Civc Tower. For both approaches, with different behavioral models and standard deviations, the results are deemed to be satisfactory considering only the approach with value of standard deviation of 0.5 where the absolute value of error is at 2% (and under) for each behavioral model. The approach with standard deviation value of 0.2 has a permittable value of error for the isotropic behavioral model, although the orthotropic behavioral model has an error value over the tolerance of 5%. At this point the best possible model comes from the calibration with standard deviation of 0.5.

The mode shapes of the FE model after optimization of calibrated mechanical parameters and frequency minimization for the isotropic and orthotropic behavioral models are displayed in Figs. 16 and 17. A good agreement can visually be found from each configuration in respect to the mode shapes of the EM (Fig. 5). All the mode shapes appear to have the 1st and 2nd modes as in-phase translational modes in x- and y-directions respectively, the 3rd mode is torsional, while the higher modes result as bending modes in their respective planes.

The direct validation between the EM and NM mode shapes comes through the MAC which proves the good agreement between the experimental and numerical applications.

**Table 17** MAC of the isotropic and orthotropic behavioral model with standard deviation of 0.5

| | Isotropic behavioral model | | | | | | Orthotropic behavioral model | | | | |
|---|---|---|---|---|---|---|---|---|---|---|---|
| | 2.68 (Hz) | 2.79 (Hz) | 6.96 (Hz) | 9.34 (Hz) | 10.47 (Hz) | | 2.68 (Hz) | 2.79 (Hz) | 6.96 (Hz) | 9.34 (Hz) | 10.47 (Hz) |
| 2.72 (Hz) | 99.03% | 0.16% | 7.84% | 57.77% | 0.00% | 2.68 (Hz) | 98.84% | 0.08% | 7.95% | 58.54% | 0.01% |
| 2.79 (Hz) | 0.13% | 99.03% | 0.25% | 0.88% | 36.36% | 2.79 (Hz) | 0.21% | 99.07% | 0.25% | 0.99% | 36.54% |
| 6.90 (Hz) | 1.52% | 1.32% | 97.41% | 28.80% | 6.48% | 7.06 (Hz) | 2.37% | 1.98% | 97.70% | 34.80% | 7.50% |
| 9.43 (Hz) | 52.12% | 1.43% | 33.78% | 95.04% | 2.41% | 9.47 (Hz) | 56.04% | 0.95% | 28.55% | 93.95% | 2.57% |
| 10.26 (Hz) | 0.02% | 47.43% | 9.59% | 2.71% | 91.82% | 10.37 (Hz) | 0.06% | 48.07% | 8.15% | 1.97% | 89.50% |

All the modes are very well correlated with values almost achieving unity in some instances. The interesting remark to be made is the close correlation that the matrices have with the CrossMAC matrix previously shown (Tables 6, 7 and 8) even outside the primary diagonal. This leads to the assumption that even if the overall correlation between the two approaches is not exact, the resemblance between the results confirms the validity of the baseline model created as a numerical replica of the current structure (Table 17).

## 5 Conclusions

The present work discussed the combination of methods whose primary force of measurement are the vibrations combined with uncertainty quantification and sensitivity analysis that led to the automatic updating of a masonry tower in the Province of Ascoli Piceno, in the village of Rotella. The principal characteristics of the tower, emerged through an initial survey campaign where geometry and material conditions were identified, have been used to realize a FE model, whose behavior has been analyzed under linear and non-linear methodologies. During the surveys, damages were reported and identified on the structure, that lead to an approach to model as discontinuities the damaged parts of the structure and consider them as such during the material parameter definitions and discretization. The field campaign was carried out to acquire vibrational responses of the tower against ambient noise under operational conditions. The data, was passed through pre-processing operations, analyzed using different modal estimators to extrapolate the dynamic parameters of the structure. This lead to build a stable experimental model to be used as reference for the calibration of the structure. Before the calibration process an uncertainty quantification followed by the definition of a surrogate model was performed. The use of such model greatly reduced the computational strain and permitted to acquire sensitivity indexes and quantify so the effect the perturbation of the material parameters of an isotropic and an orthotropic models have against the numerical dynamic responses. After seeing the results of the sensitivity analysis, it was decided to proceed considering the entirety of the uncertain parameters for the definition of the automatic updating with a GA because the late target of this procedure is to create the baseline model to be utilized in quasi-real time applications to recognize and quantify possible damages. The approach for the calibration with a GA was done considering eigen-data projected onto the equivalent numerical model. The optimization problem was solved by applying a two-term restrictive objective function for the minimization. As the approach considered also two different behavioral models one isotropic and one orthotropic, adopted for masonry applications, it led to an increased number of parameters for the procedure. The low percentage of errors, despite the significant number of parameters, demonstrated the efficiency of the method against time-consuming manual iterative procedures or other approaches that miss global optimum solutions. Further studies and investigation are to be made regarding the modeling approaches and the automatic definition of the discretization of the tower. To completely study the effect of boundary conditions, soil-structure interactions of the Rotella Civic Tower should also be considered, providing a complete comprehension the structural behavior.

Future work will include the so-called scalability of the model. Indeed, the present paper deals with a geometrically simple structure that globally behaves as a cantilever beam with rather distinct modes. However, if a different structure is considered, for instance a palace with flexible timber floors dynamically characterized by the triggering of various local

modes, then the complexity of the problem is expected to increase to a great extent. It is interesting to point out first that, the feasibility turns out to be strongly dependent on the possibility to carry out comprehensive ambient vibration tests, which is an issue mainly related to the number of sensors that can be installed. Second, an eligible case study should be selected and full access to the structure should be considered an important issue, which is not always trivial for historical constructions. Finally, the computational burden of the GA in its application to a case where the material and geometrical complexity is much higher should be considered and investigated with care in order to have an insight into the numerical complexity and the feasibility in terms of variables involved and time required for the optimization. At present, no structures with those characteristics have been identified, so no quantitative answer over this specific devepoment can be given. It is however opinion of the authors that the potential of the GA is such as to allow the analysis of structures with a complexity that certainly is much higher than that of a masonry tower.

**Fundings** Open access funding provided by Politecnico di Milano within the CRUI-CARE Agreement. The authors declare that no funds, grants, or other support were received during the preparation of this manuscript.

**Data availability** The datasets generated during and/or analyzed during the current study are available from the corresponding author on reasonable request.

## Declarations

**Conflict of interests** The authors have no relevant financial or non-financial interests to disclose.



## References

Arwade SR, Moradi M, Louhghalam A (2010) Variance decomposition and global sensitivity for structural systems. Eng Struct 32:1–10. https://doi.org/10.1016/j.engstruct.2009.08.011

Asteris PG, Sarhosis V, Mohebkhah A, et al (2015) Numerical Modeling of Historic Masonry Structures. In: Asteris P, Plevris V (eds.) Handbook of research on seismic assessment and rehabilitation of historic structures. IGI Global, Hershey, PA, pp 213–256

Azzara RM, Girardi M, Iafolla V et al (2021) Ambient vibrations of age-old masonry towers: results of long-term dynamic monitoring in the historic centre of Lucca. Int J Archit Herit 15:5–21. https://doi.org/10.1080/15583058.2019.1695155

Bartoli G, Betti M, Vignoli A (2016) A numerical study on seismic risk assessment of historic masonry towers: a case study in San Gimignano. Bull Earthq Eng 14:1475–1518. https://doi.org/10.1007/s10518-016-9892-9

Bartoli G, Betti M, Biagini P et al (2017a) Epistemic uncertainties in structural modeling: a blind benchmark for seismic assessment of slender masonry towers. J Perform Constr Facil 31:04017067. https://doi.org/10.1061/(ASCE)CF.1943-5509.0001049

Bartoli G, Betti M, Monchetti S (2017b) Seismic risk assessment of historic masonry towers: comparison of four case studies. J Perform Constr Facil 31:04017039. https://doi.org/10.1061/(ASCE)CF.1943-5509.0001039

Baudin M, Dutfoy A, Iooss B, Popelin A-L (2015) Open TURNS: An industrial software for uncertainty quantification in simulation

Benedettini F, Dilena M, Morassi A (2015) Vibration analysis and structural identification of a curved multi-span viaduct. Mech Syst Signal Process 54–55:84–107. https://doi.org/10.1016/j.ymssp.2014.08.008

Benedettini F, de Sortis A, Milana G (2017) In field data to correctly characterize the seismic response of buildings and bridges. Bull Earthq Eng 15:643–666. https://doi.org/10.1007/s10518-016-9917-4

Bianconi F, Salachoris GP, Clementi F, Lenci S (2020) A genetic algorithm procedure for the automatic updating of FEM Based on ambient vibration tests. Sensors 20:3315. https://doi.org/10.3390/s20113315

Brincker R, Zhang L, Andersen P (2000) Modal identification from ambient responses using frequency domain decomposition. In: Proceedings of the international modal analysis conference-IMAC 1:625–630

Bru D, Ivorra S, Betti M et al (2019) Parametric dynamic interaction assessment between bells and supporting slender masonry tower. Mech Syst Signal Process 129:235–249. https://doi.org/10.1016/j.ymssp.2019.04.038

Cabboi A, Gentile C, Saisi A (2017) From continuous vibration monitoring to FEM-based damage assessment: application on a stone-masonry tower. Constr Build Mater 156:252–265. https://doi.org/10.1016/j.conbuildmat.2017.08.160

Casolo S, Milani G, Uva G, Alessandri C (2013) Comparative seismic vulnerability analysis on ten masonry towers in the coastal Po Valley in Italy. Eng Struct 49:465–490. https://doi.org/10.1016/j.engstruct.2012.11.033

Ceravolo R, Pistone G, Fragonara LZ et al (2016) Vibration-based monitoring and diagnosis of cultural heritage: a methodological discussion in three examples. Int J Archit Herit 10:375–395. https://doi.org/10.1080/15583058.2013.850554

Cheng K, Lu Z, Ling C, Zhou S (2020) Surrogate-assisted global sensitivity analysis: an overview. Struct Multidiscip Optim 61:1187–1213. https://doi.org/10.1007/s00158-019-02413-5

Chieffo N, Clementi F, Formisano A, Lenci S (2019) Comparative fragility methods for seismic assessment of masonry buildings located in Muccia (Italy). J Build Eng. https://doi.org/10.1016/j.jobe.2019.100813

Clementi F, Milani G, Ferrante A, et al (2020) Crumbling of amatrice clock tower during 2016 central Italy seismic sequence: Advanced numerical insights. Frattura ed Integrita Strutturale. https://doi.org/10.3221/IGF-ESIS.51.24

di Lorenzo G, Formisano A, Krstevska L, Landolfo R (2019) Ambient vibration test and numerical investigation on the St. Giuliano church in Poggio Picenze (L'aquila, Italy). J Civ Struct Health Monit 9:477–490. https://doi.org/10.1007/s13349-019-00346-7

Ewins DJ, Saunders H (1986) Modal testing: theory and practice. J Vib Acoust 108:109–110. https://doi.org/10.1115/1.3269294

Ferrante A, Loverdos D, Clementi F et al (2021) Discontinuous approaches for nonlinear dynamic analyses of an ancient masonry tower. Eng Struct. https://doi.org/10.1016/j.engstruct.2020.111626

Ferrante A, Schiavoni M, Bianconi F et al (2021) Influence of stereotomy on discrete approaches applied to an ancient Church in Muccia, Italy. J Eng Mech. https://doi.org/10.1061/(ASCE)EM.1943-7889.0002000

Fiorentino G, Forte A, Pagano E et al (2018) Damage patterns in the town of Amatrice after August 24th 2016 Central Italy earthquakes. Bull Earthq Eng 16:1399–1423. https://doi.org/10.1007/s10518-017-0254-z

Formisano A, Krstevska L, di Lorenzo G et al (2018) Experimental ambient vibration tests and numerical investigation on the Sidoni Palace in Castelnuovo of San Pio (L'Aquila, Italy). Int J Masonry Res Innovat 3:269. https://doi.org/10.1504/IJMRI.2018.093487

Formisano A, di Lorenzo G, Krstevska L, Landolfo R (2021) Fem model calibration of experimental environmental vibration tests on two churches hit by L'Aquila Earthquake. Int J Archit Herit 15:113–131. https://doi.org/10.1080/15583058.2020.1719233

Formisano A, Di Feo P, Grippa MR, Florio G (2010) L'Aquila earthquake: A survey in the historical centre of Castelvecchio Subequo. In: COST ACTION C26 Urban habitat constructions under catastrophic events-proceedings of the final conference. pp 371–376

Forrester AIJ, Keane AJ (2009) Recent advances in surrogate-based optimization. Prog Aerosp Sci 45:50–79. https://doi.org/10.1016/j.paerosci.2008.11.001

García-Macías E, Ierimonti L, Venanzi I, Ubertini F (2020) Comparison of surrogate models for handling uncertainties in SHM of historic buildings. In: Proceedings of XXIV AIMETA conference 2019. pp 1645–1657

Gentile C, Saisi A (2007) Ambient vibration testing of historic masonry towers for structural identification and damage assessment. Constr Build Mater 21:1311–1321. https://doi.org/10.1016/j.conbuildmat.2006.01.007

Gentile C, Saisi A (2013) Operational modal testing of historic structures at different levels of excitation. Constr Build Mater 48:1273–1285. https://doi.org/10.1016/j.conbuildmat.2013.01.013

Giordano E, Mendes N, Masciotta MG et al (2020) Expeditious damage index for arched structures based on dynamic identification testing. Constr Build Mater. https://doi.org/10.1016/j.conbuildmat.2020.120236

Girardi M, Padovani C, Pellegrini D et al (2020) Finite element model updating for structural applications. J Comput Appl Math 370:112675. https://doi.org/10.1016/j.cam.2019.112675

Girardi M, Padovani C, Pellegrini D, Robol L (2021) A finite element model updating method based on global optimization. Mech Syst Signal Process 152:107372. https://doi.org/10.1016/j.ymssp.2020.107372

Jacobsen NJ, Andersen P, Brinker R (2006) Using Enhanced Frequency Domain Decomposition as a Robust Technique to Harmonic Excitation in Operational Modal Analysis. In: ISMA2006: International Conference on Noise and Vibration Engineering, Katholieke Universiteit. Leuven (Belgium)

Kita A, Cavalagli N, Ubertini F (2019) Temperature effects on static and dynamic behavior of Consoli Palace in Gubbio, Italy. Mech Syst Signal Process 120:180–202. https://doi.org/10.1016/j.ymssp.2018.10.021

Lagomarsino S, Cattari S (2015) PERPETUATE guidelines for seismic performance-based assessment of cultural heritage masonry structures. Bull Earthq Eng 13:13–47. https://doi.org/10.1007/s10518-014-9674-1

Lejeune E (2021) Geometric stability classification: datasets, metamodels, and adversarial attacks. Comput Aided Design 131:102948. https://doi.org/10.1016/j.cad.2020.102948

Magalhães F, Cunha Á, Caetano E (2009) Online automatic identification of the modal parameters of a long span arch bridge. Mech Syst Signal Process 23:316–329. https://doi.org/10.1016/j.ymssp.2008.05.003

Milani G, Clementi F (2021) Advanced seismic assessment of four masonry bell towers in italy after operational modal analysis (OMA) identification. Int J Archit Herit. https://doi.org/10.1080/15583058.2019.1697768

Milani G, Casolo S, Naliato A, Tralli A (2012) Seismic assessment of a medieval masonry tower in Northern Italy by limit, nonlinear static, and full dynamic analyses. Int J Archit Herit. https://doi.org/10.1080/15583058.2011.588987

Ministero delle infrastrutture e dei trasporti (2019) Circolare 21 gennaio 2019 n. 7 C.S.LL.PP. Istruzioni per l'applicazione dell'aggiornamento delle "Norme Tecniche per le Costruzioni" di cui al D.M. 17/01/2018 (in Italian). Suppl ord alla GU n 35 del 11/2/19

Pallarés FJ, Betti M, Bartoli G, Pallarés L (2021) Structural health monitoring (SHM) and Nondestructive testing (NDT) of slender masonry structures: a practical review. Constr Build Mater 297:123768. https://doi.org/10.1016/j.conbuildmat.2021.123768

Pastor M, Binda M, Harčarik T (2012) Modal assurance criterion. Procedia Eng 48:543–548. https://doi.org/10.1016/j.proeng.2012.09.551

Peeters B, de Roeck G (1999) Reference-based stochastic subspace identification for output-only modal analysis. Mech Syst Signal Process 13:855–878. https://doi.org/10.1006/mssp.1999.1249

Pellegrini D, Girardi M, Lourenço PB et al (2018) Modal analysis of historical masonry structures: linear perturbation and software benchmarking. Constr Build Mater 189:1232–1250. https://doi.org/10.1016/j.conbuildmat.2018.09.034

Pierdicca A, Clementi F, Fortunati A, Lenci S (2019) Tracking modal parameters evolution of a school building during retrofitting works. Bulletin Earthquake Eng. https://doi.org/10.1007/s10518-018-0483-9

Poiani M, Gazzani V, Clementi F, et al (2018) Iconic crumbling of the clock tower in Amatrice after 2016 central Italy seismic sequence: Advanced numerical insight. In: Procedia Structural Integrity

Queipo NV, Haftka RT, Shyy W et al (2005) Surrogate-based analysis and optimization. Progress Aerospace Sci 41:1–28. https://doi.org/10.1016/j.paerosci.2005.02.001

Sacks J, Welch WJ, Mitchell TJ, Wynn HP (1989) Design and analysis of computer experiments. Stat Sci. https://doi.org/10.1214/ss/1177012413

Saisi A, Gentile C, Guidobaldi M (2015) Post-earthquake continuous dynamic monitoring of the Gabbia Tower in Mantua, Italy. Constr Build Mater 81:101–112. https://doi.org/10.1016/j.conbuildmat.2015.02.010

Saisi A, Gentile C, Ruccolo A (2016) Pre-diagnostic prompt investigation and static monitoring of a historic bell-tower. Constr Build Mater 122:833–844. https://doi.org/10.1016/j.conbuildmat.2016.04.016

Salachoris GP, Magagnini E, Clementi F (2021) Mechanical characterization of "Scaglia Rossa" stone masonry through experimental and numerical analyses. Constr Build Mater. https://doi.org/10.1016/j.conbuildmat.2021.124572

Saltelli A (2002) Making best use of model evaluations to compute sensitivity indices. Comput Phys Commun 145:280–297. https://doi.org/10.1016/S0010-4655(02)00280-1

Sarhosis V, Lemos JV (2018) A detailed micro-modelling approach for the structural analysis of masonry assemblages. Comput Struct 206:66–81. https://doi.org/10.1016/j.compstruc.2018.06.003

Sarhosis V, Milani G, Formisano A, Fabbrocino F (2018) Evaluation of different approaches for the estimation of the seismic vulnerability of masonry towers. Bulletin Earthquake Eng. https://doi.org/10.1007/s10518-017-0258-8

Sarhosis V, Lemos JV, Bagi K (2019) Discrete element modeling. In: Numerical Modeling of Masonry and Historical Structures. Elsevier, pp 469–501

Standoli G, Giordano E, Milani G, Clementi F (2021a) Model updating of historical belfries based on Oma identification techniques. Int J Archit Herit. https://doi.org/10.1080/15583058.2020.1723735

Standoli G, Salachoris GP, Masciotta MG, Clementi F (2021b) Modal-based FE model updating via genetic algorithms: Exploiting artificial intelligence to build realistic numerical models of historical structures. Constr Build Mater 303:124393. https://doi.org/10.1016/j.conbuildmat.2021b.124393

Standoli G, Giordano E, Milani G, Clementi F (2020) Model Updating of Historical Belfries Based on Oma Identification Techniques. Int J Archit Herit 1–25. https://doi.org/10.1080/15583058.2020.1723735

Sun Q, Dias D (2021) Global sensitivity analysis of probabilistic tunnel seismic deformations using sparse polynomial chaos expansions. Soil Dyn Earthquake Eng 141:106470. https://doi.org/10.1016/j.soildyn.2020.106470

Torres W, Almazán JL, Sandoval C, Boroschek R (2017) Operational modal analysis and FE model updating of the Metropolitan Cathedral of Santiago, Chile. Eng Struct 143:169–188. https://doi.org/10.1016/j.engstruct.2017.04.008

Ubertini F, Comanducci G, Cavalagli N (2016) Vibration-based structural health monitoring of a historic bell-tower using output-only measurements and multivariate statistical analysis. Struct Health Monitor Int J 15:438–457. https://doi.org/10.1177/1475921716643948

Ubertini F, Comanducci G, Cavalagli N et al (2017) Environmental effects on natural frequencies of the San Pietro bell tower in Perugia, Italy, and their removal for structural performance assessment. Mech Syst Signal Process 82:307–322. https://doi.org/10.1016/j.ymssp.2016.05.025

Ubertini F, Cavalagli N, Kita A, Comanducci G (2018) Assessment of a monumental masonry bell-tower after 2016 Central Italy seismic sequence by long-term SHM. Bull Earthq Eng 16:775–801. https://doi.org/10.1007/s10518-017-0222-7

Zini G, Betti M, Bartoli G (2022) A quality-based automated procedure for operational modal analysis. Mech Syst Signal Process 164:108173. https://doi.org/10.1016/j.ymssp.2021.108173